

Zero modes and edge states of the honeycomb lattice

Mahito Kohmoto¹ and Yasumasa Hasegawa²

¹*Institute for Solid State Physics, University of Tokyo, 5-1-5 Kashiwanoha, Kashiwa, Chiba 277-8581, Japan*

²*Department of Material Science, Graduate School of Material Science, University of Hyogo Ako, Hyogo 678-1297, Japan*

(Received 6 February 2007; revised manuscript received 30 April 2007; published 2 November 2007)

The honeycomb lattice in the cylinder geometry with zigzag edges, bearded edges, zigzag and bearded edges (zigzag-bearded), and armchair edges are studied. The tight-binding model with nearest-neighbor hoppings is used. Edge states are obtained analytically for these edges except the armchair edges. It is shown, however, that edge states for the armchair edges exist when the system is anisotropic. These states have not been known previously. We also find strictly localized states, uniformly extended states, and states with macroscopic degeneracy.

DOI: 10.1103/PhysRevB.76.205402

PACS number(s): 73.43.-f, 71.10.Pm, 71.10.Fd

I. INTRODUCTION

Monolayer graphite, called graphene, was fabricated recently¹⁻³ and novel physical properties have been expected to be seen. In fact, integer quantum Hall effect^{1,2} has been observed.

In this paper, we report a systematic study of the zero modes and the corresponding edge states of the honeycomb lattice which is shown in Fig. 1. The cylindrical geometry is taken and thus two edges are present. We consider three types of edges, zigzag, bearded, and armchair, which are shown in Fig. 2. Two edges of the same type can form a cylinder. In addition, zigzag and bearded edges can form a cylinder. We call these zigzag, bearded, armchair, and zigzag-bearded, respectively. An armchair edge and a zigzag edge (or a bearded edge) cannot form a pair of edges for a cylinder. When only nearest-neighbor hoppings are taken, the zero-energy edge states for zigzag, bearded, and zigzag-bearded are obtained. They are localized near the edges with the localization length

$$\xi = \frac{1}{2|\log t|}, \quad (1)$$

where

$$t = \sqrt{2(1 + \cos k_y)} = 2 \left| \cos \frac{k_y}{2} \right| \quad (2)$$

and k_y is the reciprocal lattice vector in the y direction. We find the uniformly extended states at $|k_y| = \frac{2\pi}{3}$, as well as the strictly localized states at $|k_y| = \pi$. In addition, the origin of the states with macroscopic degeneracy at $|k_y| = \pi$ with $E = \pm 1$ is explained.

The localization length of armchair diverges and there are no edge states if it is isotropic. We find edge states, however, if the system is anisotropic, i.e., three hoppings t_a , t_b , and t_c are not equal.^{4,5}

Some of our results have been reported previously in the tight-binding model,⁶⁻¹³ the effective Dirac equation,¹⁴⁻¹⁶ and the first principles calculations.¹⁷⁻²² For the isotropic tight-binding model, Klein⁶ has obtained the condition for the existence of the edge states for the bearded edge. Fujita *et al.*⁷ obtained the conditions for the zigzag and armchair edges. However, there have been no studies of the aniso-

tropic cases. Due to the massless Dirac model, the Jahn-Teller effect could take place in this system. The spontaneous breaking of the lattice symmetry would give rise to the anisotropic cases.

II. TIGHT-BINDING MODEL

Zigzag, bearded, zigzag-bearded, and armchair are shown in Figs. 2(a)–2(d). We pair a site on sublattice A and a site on sublattice B and denote the wave functions of a pair as $\psi_{n,m}$ and $\phi_{n,m}$, as shown in Fig. 1, where n and m are both integers or both half-integers. Then, nearest-neighbor hoppings give a tight-binding model,

$$\begin{aligned} -t_a \psi_{n,m} - t_b \psi_{n+1/2,m-1/2} - t_c \psi_{n+1/2,m+1/2} &= E \phi_{n,m}, \\ -t_a \phi_{n,m} - t_b \phi_{n-1/2,m+1/2} - t_c \phi_{n-1/2,m-1/2} &= E \psi_{n,m}, \end{aligned} \quad (3)$$

where t_a is an intrapair hopping between $\psi_{n,m}$ and $\phi_{n,m}$ and t_b and t_c are interpair hoppings.

III. ZIGZAG AND BEARDED

The zigzag edge and bearded edge can appear in the left edge or right edge. If the left edge is formed by sublattice A or B, it is bearded or zigzag, respectively. If the right edge is

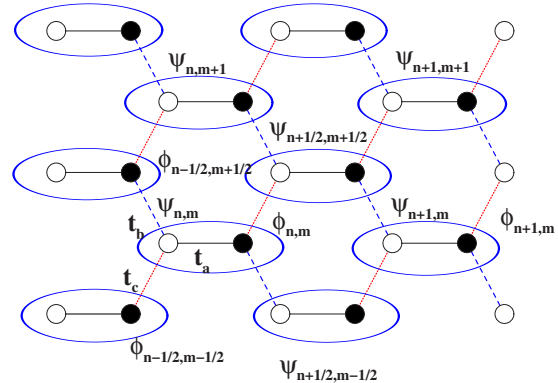


FIG. 1. (Color online) The honeycomb lattice. The open and closed circles show sublattices A and B, respectively. The wave functions are $\phi_{n,m}$, $\phi_{n+1/2,m+1/2}$, $\psi_{n,m}$, and $\psi_{n+1/2,m+1/2}$, where n and m are both integers or both half-integers. Hoppings are t_a , t_b , and t_c .

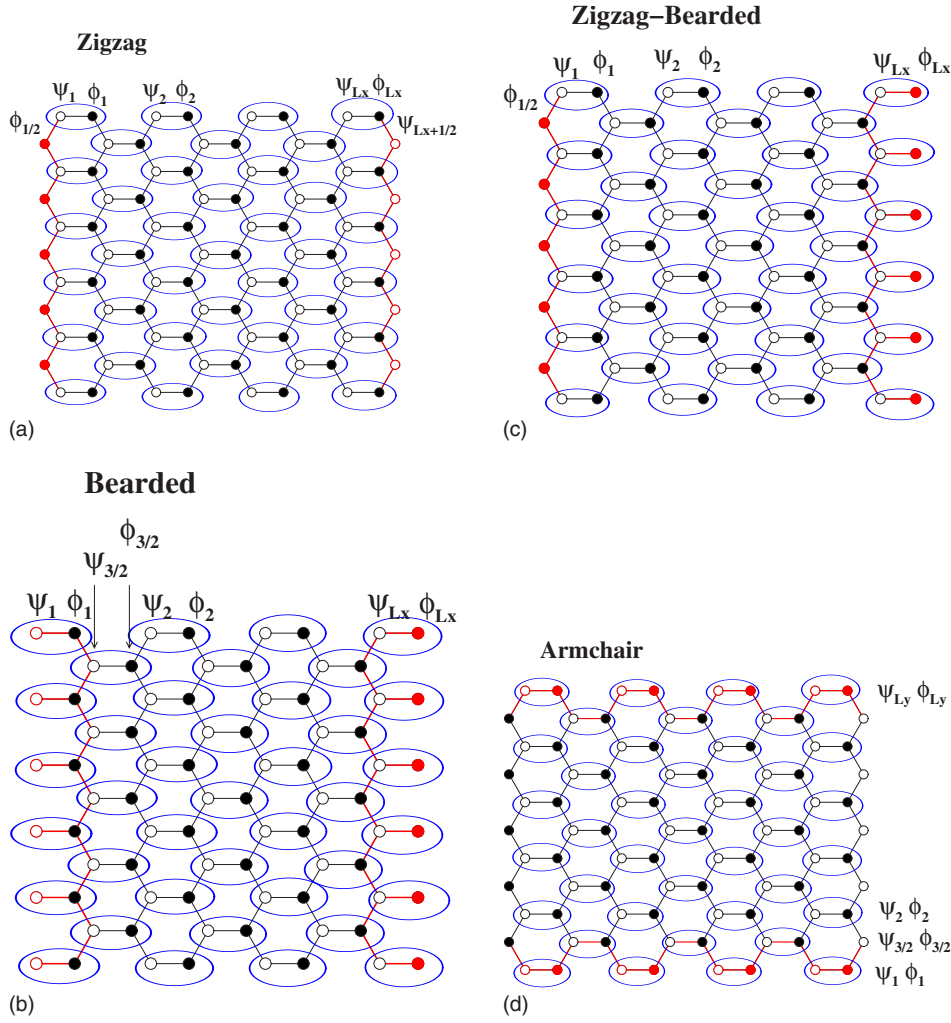


FIG. 2. (Color online) The honeycomb lattices with (a) zigzag ($L_x=4$), (b) bearded ($L_x=4$), (c) zigzag-bearded ($L_x=4$), and (d) armchair ($L_y=6$) edges, which we call zigzag, bearded, zigzag-bearded, and armchair, respectively.

formed by sublattice A or B, it is zigzag or bearded, respectively.

We have edges in the y direction, as shown in Figs. 2(a)–2(c) and impose the periodic boundary conditions $\psi_{n,m+L_y} = \psi_{n,m}$ and $\phi_{n,m+L_y} = \phi_{n,m}$ in the y direction, where L_y is an integer. Then, one can write

$$\begin{aligned}\psi_{n,m} &= \exp(ik_y m) \psi_n \\ \phi_{n,m} &= \exp(ik_y m) \phi_n,\end{aligned}\quad (4)$$

where $k_y = \frac{2\pi j}{L_y}$ and $j=1, \dots, L_y$ and Eq. (3) is written as

$$\begin{aligned}\psi_n + t_1 \psi_{n+1/2} &= -\frac{E}{t_a} \phi_n, \\ \phi_n + t_2 \phi_{n-1/2} &= -\frac{E}{t_a} \psi_n,\end{aligned}\quad (5)$$

where

$$t_1 = \frac{t_b e^{-i(k_y/2)} + t_c e^{i(k_y/2)}}{t_a}, \quad (6)$$

$$t_2 = t_1^* = \frac{t_b e^{-i(k_y/2)} + t_c e^{i(k_y/2)}}{t_a}. \quad (7)$$

We define

$$t = |t_1| = |t_2| = \frac{\sqrt{t_b^2 + t_c^2 + 2t_b t_c \cos k_y}}{t_a}. \quad (8)$$

When $t_b = t_c$, we have

$$t_1 = \frac{2t_b}{t_a} \cos \frac{k_y}{2}. \quad (9)$$

A. Macroscopically degenerate states and the strictly localized states at $t_b = t_c$ and $|k_y| = \pi$

If $t_b = t_c$ and $|k_y| = \pi$, Eqs. (6) and (7) vanish. Then Eq. (5) is

$$\psi_n = -\frac{E}{t_a} \phi_n,$$

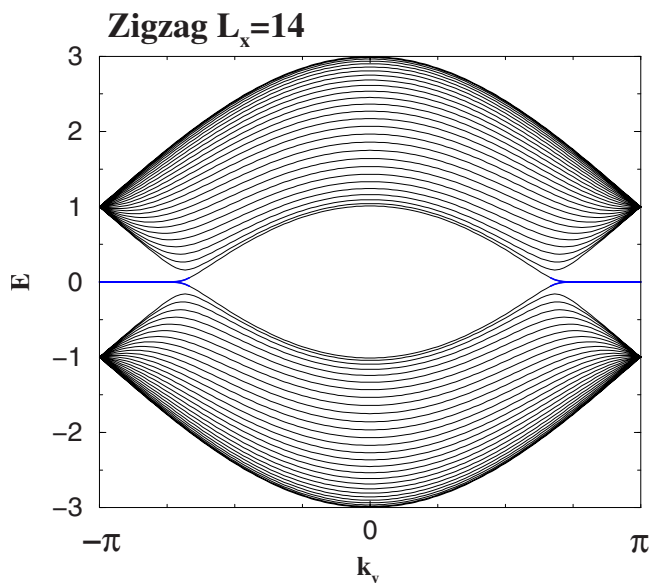


FIG. 3. (Color online) Energy spectrum of zigzag for $L_x=14$. The edge states are on the blue lines.

$$\phi_n = -\frac{E}{t_a} \psi_n. \quad (10)$$

There is no interpair coupling and each pair is decoupled from others. This leads to macroscopic degeneracy. These are bulk states which appear at $|k_y| = \pi$ and $E = \pm t_a$ for zigzag, bearded, and zigzag-bearded, as shown in Figs. 3, 5, and 6, respectively.

If we have $E=0$ in addition, pairs (ψ_n, ϕ_n) vanish, as seen from Eq. (10). The only nonvanishing wave functions are the unpaired ones at the edges. For zigzag, the unpaired wave functions are $\phi_{1/2}$ and $\psi_{L_x+1/2}$, as shown in Fig. 2(a). Thus, we have strictly localized states $\phi_{1/2}$ at the left edge and $\psi_{L_x+1/2}$ at the right edge. (These states are extended in the y direction.) For bearded, there is no unpaired state, as shown in Fig. 2(b), and there is no strictly localized state. For zigzag-bearded, ϕ_1 is unpaired, as shown in Fig. 2(c). This is the strictly localized state at the left edge. (This state is extended in the y direction.)

B. Edge states

In the following, we implicitly assume the appropriate thermodynamic limit. If $E=0$, Eq. (5) is reduced to

$$\begin{aligned} \psi_n &= -t_1 \psi_{n+1/2}, \\ \phi_n &= -t_2 \phi_{n-1/2}. \end{aligned} \quad (11)$$

There is no intrapair coupling, namely, ψ_n 's on sublattice A and ϕ_n 's on sublattice B are decoupled.

1. Zigzag

As shown in Fig. 2(a), the left edge has $\phi_{1/2}$ on sublattice B and the right edge has $\psi_{L_x+1/2}$ on sublattice A. The boundary condition on the left edge is to add fictitious sites with

$\psi_{1/2}=0$. In the same manner, the boundary condition on the right edge is to add fictitious sites with $\phi_{L_x+1/2}=0$. Thus, the boundary conditions for zigzag are

$$\psi_{1/2} = 0, \quad (12)$$

$$\phi_{L_x+1/2} = 0. \quad (13)$$

From Eqs. (10) and (11), we obtain

$$\psi_{L_x-n} = (-t_1)^{2n+1/2} \psi_{L_x+1/2}, \quad (14)$$

$$\phi_n = (-t_2)^{2n-1} \phi_{1/2}. \quad (15)$$

For the system with finite L_x , the solutions above are not exact. If $t < 1$, however, Eqs. (14) and (15) satisfy the boundary conditions in the limit $L_x \rightarrow \infty$ and these give the right edge states on sublattice A and the left edge states on sublattice B, respectively. Even if the system size is finite, we have the edge states with exponentially small E , when the edge states on sublattices A and B coexist with negligibly small mixing to satisfy the exact boundary conditions.

The localization lengths for both sublattices are the same and given by

$$\xi = \frac{1}{2|\log t|}. \quad (16)$$

From Eq. (8), the condition for the existence of the edge states, $t < 1$, is given by

$$\cos k_y < \frac{t_a^2 - t_b^2 - t_c^2}{2t_b t_c}. \quad (17)$$

Thus we have edge states for all the values of k_y if $t_b + t_c < t_a$. There are no edge states if $|t_b - t_c| > t_a$.

For $t_a = t_b = t_c$, edge states exist if $|k_y| > \frac{2\pi}{3}$. The zero energy modes for these edge states are seen in Fig. 3. An example of edge states are shown in Fig. 4.

2. Bearded

As shown in Fig. 2(b), the left edge has ψ_1 on sublattice A and the right edge has ϕ_{L_x} on sublattice B. The boundary conditions are given by

$$\begin{aligned} \psi_{L_x+1/2} &= 0, \\ \phi_{1/2} &= 0. \end{aligned} \quad (18)$$

In this case, we write Eq. (11) as

$$\begin{aligned} \psi_n &= \left(-\frac{1}{t_1}\right)^{2n-2} \psi_1, \\ \phi_{L_x-n} &= \left(-\frac{1}{t_2}\right)^{2n} \phi_{L_x}. \end{aligned} \quad (19)$$

If $t > 1$, these are edge states with the same localization length

$$\xi = \frac{1}{2 \log t}. \quad (20)$$

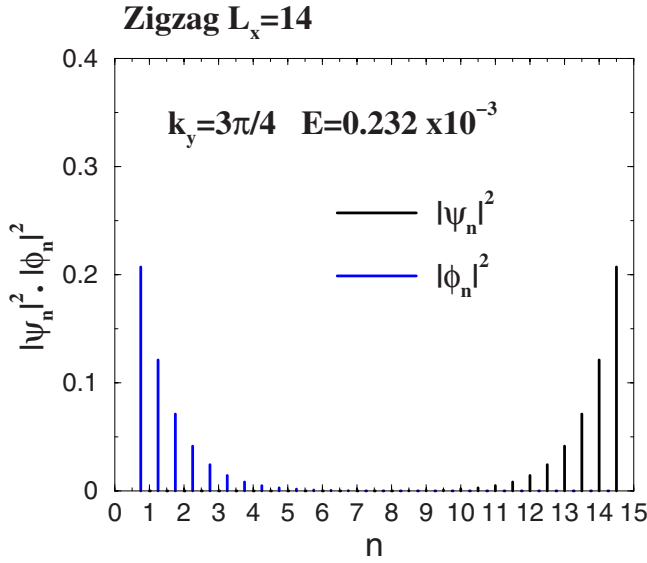


FIG. 4. (Color online) An example of the edge states.

For $t_a=t_b=t_c$, edge states exist if $|k_y| < \frac{2\pi}{3}$. The energy spectrum for the isotropic case is plotted in Fig. 5.

3. Zigzag-bearded

As shown in Fig. 2(c), the left edge is zigzag with $\phi_{1/2}$ on sublattice B. The right edge is bearded with ϕ_{L_x} also on sublattice B. The boundary conditions are given by

$$\psi_{1/2} = 0, \quad (21)$$

$$\psi_{L_x+1/2} = 0. \quad (22)$$

These boundary conditions give $\psi_n=0$. Thus, there are no edge states on sublattice A.

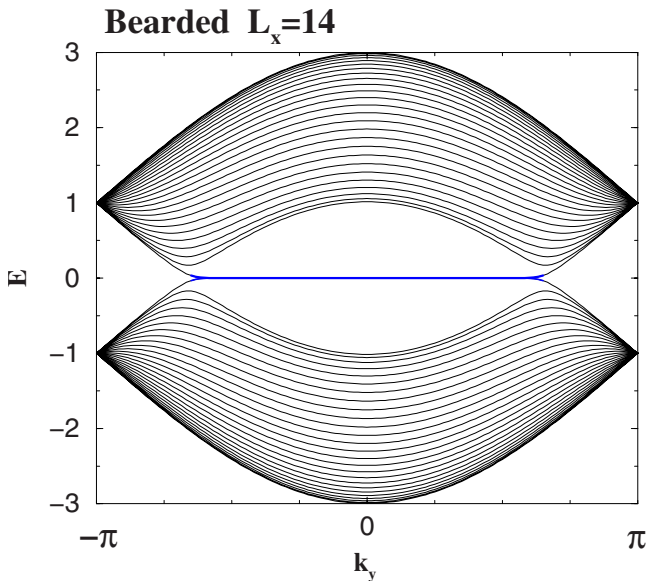
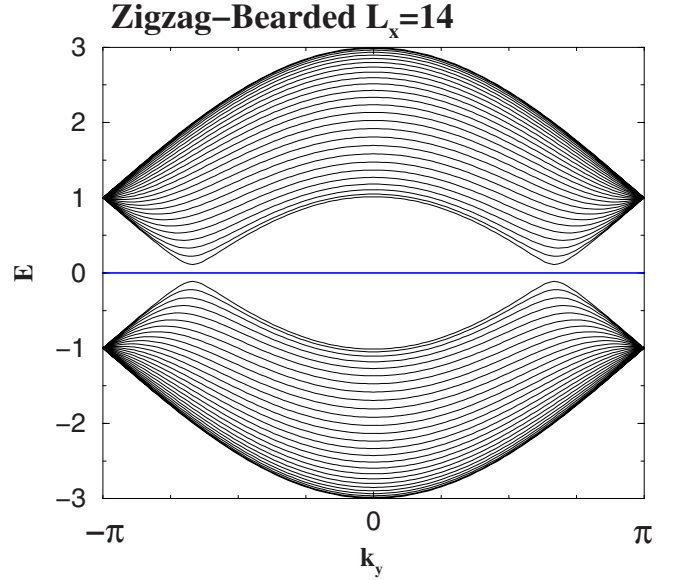


FIG. 5. (Color online) Energy spectrum for bearded. The energy mode for the edge states are on the blue line.


 FIG. 6. (Color online) Energy spectrum for zigzag-bearded for $L_x=40$. The zero energy mode for the edge states are on the blue line.

For the ϕ_n , we have no boundary conditions. From Eq. (11), we have

$$\phi_n = (-t_2)^{2n-1} \phi_{1/2}, \quad (23)$$

This is the left edge states if $t < 1$. On the other hand, we write

$$\phi_{L_x-n} = \left(-\frac{1}{t_2}\right)^{2n} \phi_{L_x}, \quad (24)$$

This gives the right edge state if $t > 1$.

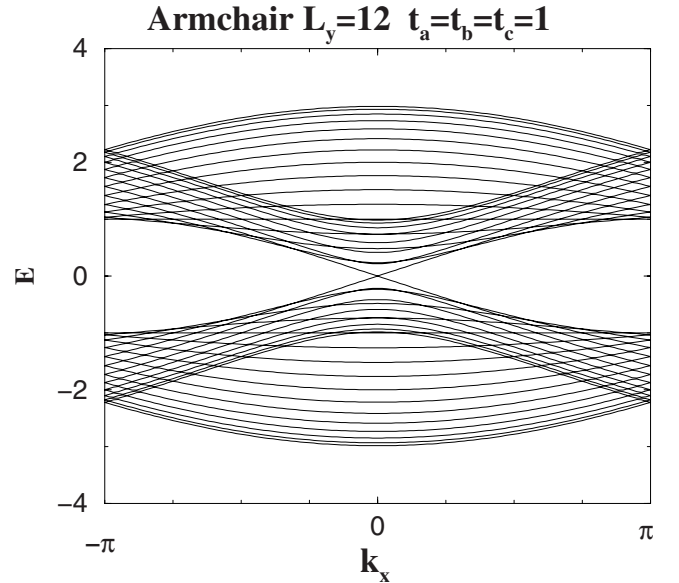


FIG. 7. (Color online) Energy spectrum for armchair in the isotropic case. Neither Eq. (31) nor Eq. (33) is satisfied in this case. There is no edge state.

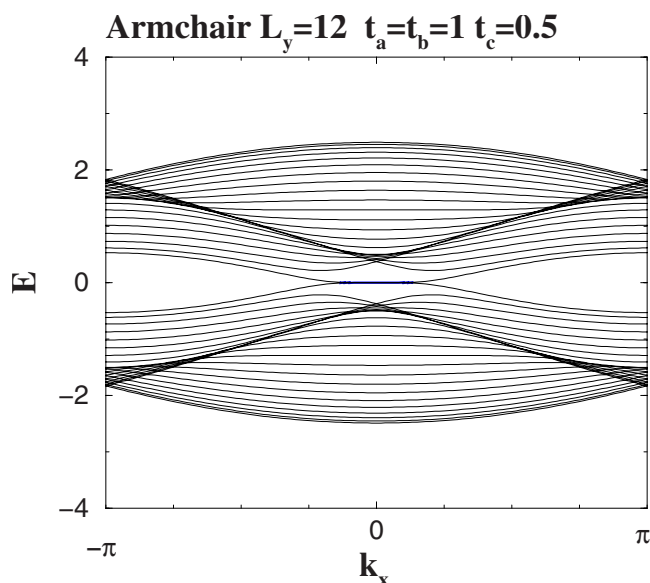


FIG. 8. (Color online) Energy spectrum for armchair in an anisotropic case. The condition Eq. (33) is satisfied for certain k_x 's and edge states exist on the blue line.

The energy spectrum in the isotropic case, $t_a=t_b=t_c$, is shown in Fig. 6. The edge states are on the blue line which has the full length from $-\pi$ to π .

IV. ARMCHAIR

We have the periodic boundary conditions in the x -direction, $\psi_{n+L_x,m}=\psi_{n,m}$ and $\phi_{n+L_x,m}=\phi_{n,m}$, as shown in Fig. 2(d). So, we write

$$\begin{aligned}\psi_{n,m} &= \exp(ik_x n)\psi_m, \\ \phi_{n,m} &= \exp(ik_x n)\phi_m,\end{aligned}\quad (25)$$

where $k_x = \frac{2\pi j}{L_x}$ and $j=1, \dots, L_x$. The boundary conditions at the edges are

$$\begin{aligned}\psi_{1/2} &= \phi_{1/2} = 0, \\ \psi_{L_y+1/2} &= \phi_{L_y+1/2} = 0.\end{aligned}\quad (26)$$

Let us consider the case where $E=0$ in which ψ 's and ϕ 's are decoupled and satisfy

$$-t_a\psi_m - e^{i(k_x/2)}(t_b\psi_{m-1/2} + t_c\psi_{m+1/2}) = 0,$$

$$-t_a\phi_m - e^{-i(k_x/2)}(t_b\phi_{m+1/2} + t_c\phi_{m-1/2}) = 0. \quad (27)$$

We set

$$\psi_m = z^{2m}. \quad (28)$$

Then, from Eq. (27), we have two solutions for z which satisfy

$$\begin{aligned}z_{\pm} &= \frac{1}{2} \left[-\frac{t_a}{t_c} e^{-ik_x/2} \pm \sqrt{\left(\frac{t_a}{t_c}\right)^2 e^{-ik_x} - 4\frac{t_b}{t_c}} \right], \\ z_{\pm} z_{\mp} &= \frac{t_b}{t_c}, \\ z_+ + z_- &= -\frac{t_a}{t_c} e^{-ik_x/2},\end{aligned}\quad (29)$$

In terms of these, the solution of Eq. (27) with the boundary condition $\psi_{1/2}=0$ is given by

$$\psi_m = \frac{z_+^{2m-1} - z_-^{2m-1}}{z_+ - z_-} \psi_1. \quad (30)$$

This satisfies the boundary condition in the limit $L_y \rightarrow \infty$ if

$$|z_+| < 1 \text{ and } |z_-| < 1. \quad (31)$$

They are edge states localized near the bottom. In order Eq. (31) be satisfied,

$$t_b < t_c, \quad (32)$$

is required as seen from Eq. (29).

In a similar manner, edge states localized near the top are possible if

$$|z_+| > 1 \text{ and } |z_-| > 1 \quad (33)$$

As seen from Eq. (29)

$$t_b > t_c, \quad (34)$$

is required.

For analysis of ϕ 's we only need to replace k_x by $-k_x$ and t_b and t_c . This symmetry can be seen in Fig. 1 and also in Eq. (27). Thus we obtain essentially the same conditions. See Figs. 7 and 8 for examples of the energy spectrum.

ACKNOWLEDGMENT

We thank T. Aoyama for help with a computer calculation.

¹K. S. Novoselov, A. K. Geim, S. V. Morozov, D. Jiang, M. I. Katsnelson, I. V. Grigorieva, S. V. Dubonos, and A. A. Firsov, *Nature (London)* **438**, 197 (2005).

²Y. Zhang, Y.-W. Tan, H. Stormer, and P. Kim, *Nature (London)* **438**, 201 (2005).

³C. Berger *et al.*, *Science* **312**, 1191 (2006).

⁴Y. Hasegawa, R. Konno, H. Nakano, and M. Kohmoto, *Phys.*

Rev. B **74**, 033413 (2006).

⁵Y. Hasegawa and M. Kohmoto, *Phys. Rev. B* **74**, 155415 (2006).

⁶D. J. Klein, *Chem. Phys. Lett.* **217**, 261 (1994).

⁷M. Fujita, K. Wakabayashi, K. Nakada, and K. Kusakabe, *J. Phys. Soc. Jpn.* **65**, 1920 (1996).

⁸K. Nakada, M. Fujita, G. Dresselhaus, and M. S. Dresselhaus, *Phys. Rev. B* **54**, 17954 (1996).

- ⁹K. Wakabayashi, M. Fujita, H. Ajiki, and M. Sigrist, *Phys. Rev. B* **59**, 8271 (1999).
- ¹⁰K. Kusakabe and Y. Takagi, *Mol. Cryst. Liq. Cryst. Sci. Technol., Sect. A* **387**, 7 (2002).
- ¹¹S. Ryu and Y. Hatsugai, *Phys. Rev. Lett.* **89**, 077002 (2002).
- ¹²M. Ezawa, *Phys. Rev. B* **73**, 045432 (2006).
- ¹³N. M. R. Peres, F. Guinea, and A. H. Castro Neto, *Phys. Rev. B* **73**, 125411 (2006).
- ¹⁴L. Brey and H. A. Fertig, *Phys. Rev. B* **73**, 235411 (2006).
- ¹⁵K. Sasaki, S. Murakami, and R. Saito, *J. Phys. Soc. Jpn.* **75**, 074713 (2006).
- ¹⁶D. A. Abanin, P. A. Lee, and L. S. Levitov, *Phys. Rev. Lett.* **96**, 176803 (2006).
- ¹⁷Y. Miyamoto, K. Nakada, and M. Fujita, *Phys. Rev. B* **59**, 9858 (1999).
- ¹⁸S. Okada and A. Oshiyama, *Phys. Rev. Lett.* **87**, 146803 (2001).
- ¹⁹S. Okada and A. Oshiyama, *J. Phys. Soc. Jpn.* **72**, 1510 (2003).
- ²⁰H. Lee, Y. W. Son, N. Park, S. Han, and J. Yu, *Phys. Rev. B* **72**, 174431 (2005).
- ²¹Y. W. Son, M. L. Cohen, and S. G. Louie, *Phys. Rev. Lett.* **97**, 216803 (2006).
- ²²Y. W. Son, M. L. Cohen, and S. G. Louie, *Nature (London)* **444**, 347 (2006).